https://dx.doi.org/10.4314/dujopas.v10i3b.19
ISSN (Print): 2476-8316
ISSN (Online): 2635-3490
Dutse Journal of Pure and Applied Sciences (DUJOPAS), *Vol. 10 No. 3b September 2024*

Numerical Solution of Fractional Order Model of Measles Disease with Double Dose Vaccination

Agbata, B.C.[1], Obeng-Denteh, W[2], Amoah-Mensah, J[3], Kwabi, P. A[2], Shior, M.M[4], Asante Mensa, F[2], Abraham, S[5]

[1]Department of Mathematics and Statistics,
Faculty of Science,
Confluence University of Science and Technology,
Osara,
Nigeria.

[2]Department of Mathematics,
College of Science,
Kwame Nkrumah University of Science and Technology,
Kumasi,
Ghana.

[3]Sunyani Technical University,
Sunyani,
Ghana.

[4]Department of Mathematics/ Computer Science,
Benue State University,
Makurdi,
Nigeria.

[5]Department of Mathematics, School of Sciences,
Federal College of Education (Technical),
Ekiadolor,
Nigeria.

Abstract

Measles remains a significant public health concern globally, despite the availability of effective vaccines. In this study, we develop a mathematical model of measles disease that integrates the impact of double dose vaccination and utilize the Laplace Adomian Decomposition Method (LADM) as a numerical approach to obtain solutions for the fractional order differential equations governing the model. The model accounts for the dynamics of susceptible, infected, and vaccinated individuals, considering the transmission dynamics of measles in a population with varying vaccination coverage. LADM, combining the Laplace transform and Adomian decomposition, provides a systematic method to solve the nonlinear fractional differential equations derived from the model, offering insights into the effectiveness of double dose vaccination strategies in controlling measles outbreaks.

Keywords: Measles, Mathematical modelling, Infectious Disease, Approximate Solution, Double Vaccinations.

Author for Correspondence

INTRODUCTION

Measles, caused by the measles virus (MeV), is an extremely contagious respiratory infection that primarily affects children and unvaccinated individuals. Symptoms include fever, cough, runny nose, and a distinctive rash that starts on the face and spreads. Despite the availability of an effective vaccine, measles remains a significant global health concern, causing considerable illness and mortality, particularly in areas with low vaccination rates (NCDC, 2023). The measles virus belongs to the Paramyxoviridae family, specifically the Morbillivirus genus. It spreads through respiratory droplets or direct contact with infected nasal or throat secretions (WHO, 2021). After an incubation period of 7 to 14 days, infected individuals can transmit the virus, contributing to outbreaks, especially in communities with low vaccination coverage (WHO, 2021).Before widespread vaccination, measles was common worldwide. The introduction of the measles vaccine, typically administered as part of the *Measles-Mumps-Rubella (MMR)* series, has led to a significant decrease in global measles (NCDC, 2023). However, outbreaks still occur due to vaccine hesitancy and incomplete vaccination coverage, highlighting the need for sustained immunization efforts to achieve herd immunity (WHO, 2021).Measles can lead to severe complications, particularly in young children and those with compromised immune systems, such as pneumonia, encephalitis, and ear infections (NCDC, 2023). Pregnant women infected with measles are also at risk of complications, including miscarriage and premature birth (WHO, 2021). The high contagiousness and potential for severe outcomes underscore the importance of vaccination and public health measures to prevent and control measles outbreaks globally.

The Laplace Adomian Decomposition Method (LADM) is a powerful numerical technique used to solve differential equations, including fractional-order models, by combining the Laplace transform and Adomian decomposition method (ADM). Introduced as an extension of the classical Adomian decomposition method by (Jafari and Daftardar-Gejji, 2006). LADM offers a systematic approach to solving nonlinear problems that involve fractional derivatives. In LADM, the Laplace transform is first applied to the differential equation, transforming it into an algebraic equation in the Laplace domain. The resulting equation is then decomposed into a series using the Adomian polynomials. These polynomials represent the nonlinear terms of the original equation and are recursively computed to approximate the solution in terms of a series.

The method's strength lies in its ability to handle nonlinearities and fractional derivatives efficiently, making it particularly suitable for modeling complex phenomena such as fractional-order differential equations encountered in epidemiology, finance, physics, and engineering (Jafari and Daftardar-Gejji, 2006). By decomposing the problem into simpler components and using iterative techniques, LADM provides a systematic framework for obtaining numerical solutions that are often challenging to derive analytically. Applications of LADM range from solving differential equations governing infectious disease dynamics, such as measles spread models with fractional-order terms, to financial models involving fractional calculus. Its flexibility and computational efficiency make LADM a valuable tool in both theoretical studies and practical applications where traditional analytical methods may be insufficient.

Using the Laplace Adomian Decomposition Method (LADM) offers several benefits, making it a valuable numerical technique for solving differential equations, particularly those involving fractional derivatives. Here are some benefits of using LADM:

- **Suitability for Fractional Calculus Problems:**LADM is specifically designed to handle fractional-order differential equations, which often arise in various scientific and engineering disciplines. These equations involve derivatives of non-integer order,

and LADM provides a systematic approach to obtaining numerical solutions for such complex problems (Jafari and Daftardar-Gejji, 2006).

- **Systematic Decomposition of Nonlinear Terms:** The method decomposes the nonlinear terms of the differential equation into a series of Adomian polynomials. This decomposition simplifies the solution process by breaking down the problem into manageable components, facilitating iterative computation and convergence (Jafari and Daftardar-Gejji, 2006).
- **Efficiency in Handling Nonlinearities:** LADM efficiently handles nonlinear differential equations, which are often challenging to solve using traditional analytical methods. By decomposing the nonlinear terms and applying iterative techniques, LADM provides accurate approximations of the solution without the need for linearization or simplification of the original equation (Jafari and Daftardar-Gejji, 2006).
- **Convergence and Accuracy:** The method typically exhibits good convergence properties when applied to well-posed problems. Through iterative refinement of the Adomian series, LADM can achieve accurate numerical solutions that closely approximate the true solution of the differential equation. This accuracy is crucial for modeling and predicting real-world phenomena with fractional dynamics (Jafari and Daftardar-Gejji, 2006).
- **Flexibility and Applicability Across Disciplines:** LADM's versatility allows it to be applied across various scientific and engineering fields, including epidemiology, finance, physics, and chemical engineering. It can handle a wide range of differential equations with fractional derivatives, making it a preferred choice for researchers and practitioners dealing with complex nonlinear systems (Jafari and Daftardar-Gejji, 2006).
- **Integration with Computational Tools**:The method can be implemented using computational software packages, enhancing its practical utility in solving real-world problems. Researchers and engineers can leverage existing numerical libraries and programming environments to apply LADM to their specific applications, thereby streamlining the solution process and improving productivity (Jafari and Daftardar-Gejji, 2006). The Laplace Adomian Decomposition Method (LADM) offers significant advantages in solving fractional-order differential equations, including systematic handling of nonlinearities, efficiency in computation, accuracy of solutions, and broad applicability across disciplines.

Several authors have studied mathematical modeling of infectious diseases with vaccination strategies.

Thompson & Andrews (2023), studied mathematical modelling of measles transmission and vaccination strategies: Their study considered various mathematical models used to analyze measles transmission dynamics and vaccination strategies. Thompson and Andrews discussed the impacts of vaccination coverage, vaccine efficacy, and population characteristics on measles epidemiology. They highlighted critical thresholds for measles elimination and the effects of vaccine hesitancy on outbreak dynamics. The review synthesizes findings from different modeling approaches, including compartmental and agent-based models, illustrating how these models inform public health strategies to control measles globally. The authors emphasized the importance of continuous model refinement to address emerging challenges in measles eradication efforts. Metcalf & Grenfell (2022) , studied challenges and opportunities in modeling measles vaccination. This article considered the challenges and opportunities in modeling measles vaccination strategies aimed at achieving disease

elimination. Metcalf and Grenfell discussed the complexities of vaccine hesitancy, population immunity dynamics, and the impact of global vaccination campaigns on measles transmission dynamics. They highlighted the integration of behavioral and demographic factors into mathematical models to optimize vaccination coverage and effectiveness. Their study emphasized the role of mathematical modeling in guiding vaccination policies and emphasized the need for interdisciplinary collaboration to sustain global measles elimination efforts.

Shim, & Galvani (2021) , studied measles vaccination for disease control: A modeling perspective. Shim and Galvani provided a modeling perspective on measles vaccination strategies for disease control. They evaluated the impact of vaccination on measles transmission dynamics using mathematical models, exploring various vaccination scenarios and strategies. The article discussed the effectiveness of routine immunization, supplementary immunization activities, and outbreak response strategies in controlling measles outbreaks. Shim and Galvani highlighted the role of targeted vaccination campaigns in high-risk populations and the integration of vaccination with other public health interventions. They concluded by advocating for the use of mathematical modeling to inform proactive vaccination policies and optimize resource allocation for measles control efforts.Some relevant works are found in the following references Agbata et al. (2021), Ayla, (2015), Agbata et al. (2024), Acheneje et al. (2024), Chitnis et al . (2008), Okon et al. (2023). This study aims to create a mathematical model for measles that integrates the effects of double dose vaccination and solve it using the Laplace Adomian Decomposition Method (LADM). The objectives are to develop a fractional order mathematical model that includes vaccination parameters, derive the corresponding fractional differential equations, and use the Laplace transform to convert these into algebraic equations. The Adomian decomposition method will then be applied to these equations to obtain numerical solutions. Finally, the study will evaluate the impact of double dose vaccination on controlling measles outbreaks through numerical simulations and comparisons with real-world data.

Materials and Methods

Model Formulation

The total population $N(t)$, is divided into six epidemiological groups: susceptible individuals (S),, individuals who have received the first dose of vaccination but can still be infected due to vaccine failure (V_1), individuals who have completed the second dose of vaccine (V_2), exposed individuals (E), infected individuals (I), and recovered individuals (R). Let λ be the constant recruitment rate. Suppose ρ denotes the fraction of individuals who refused vaccination before entering the population, and $(1-\rho)$ represents individuals who have taken the first dose of vaccine before entering the population, where α_1 is the rate at which susceptible individuals take the first dose of vaccine, and β denotes the probability of transmission by an infected individual with measles. ω is the rate at which those who took the first dose of vaccine become exposed due to vaccine failure, and ψ denotes the rate at which initially vaccinated individuals become infected due to vaccine failure. α_2 is the rate of vaccination of initially vaccinated individuals, α_3 represents the recovery rate of vaccinated individuals, σ is the rate at which exposed individuals become infected, and f is the recovery rate of infected individuals. μ represents the natural death rate, and ε is the disease-induced death rate.

Model Assumptions

The model is developed under the following mathematical assumptions

1. Uniform Interaction: The model assumes that individuals within the population mix uniformly, meaning everyone has an equal likelihood of encountering others.
2. Stable Population Size: Throughout the model, the total population remains constant, with negligible birth and death rates over the modeled period.
3. First Vaccination Dose Group (V1): These individuals have had one dose of the measles vaccine but can still be susceptible to infection due to vaccine ineffectiveness.
4. Vaccine Effectiveness and Failures: We assumed that individuals receiving the first vaccine dose might still become exposed or infected due to vaccine failure, indicating that the vaccine isn't entirely effective after the initial dose.
5. Duration of Immunity: The model assumes that individuals who recover from measles or complete the vaccination series (two doses) gain immunity for a certain period, with the possibility of immunity waning over time.
6. Transmission Dynamics: The model follows a susceptible-infected-recovered (SIR) framework, with individuals transitioning between susceptible, infected, and recovered states based on transmission rates and probabilities.

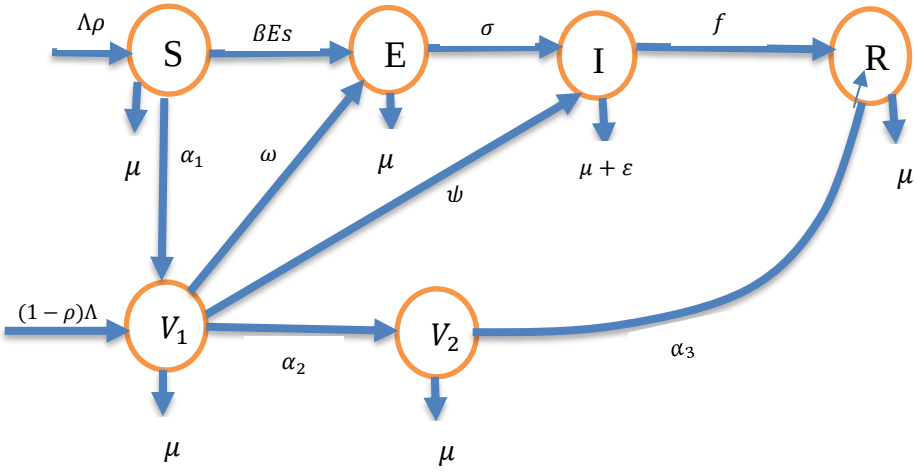

Fig: 1 Schematic diagram for the Model

Model Equation

$$
\left.
\begin{aligned}
\frac{dS}{dt} &= \Lambda\rho - (\beta E + \alpha_1 + \mu)\mathrm{S} \\
\frac{d\,\mathrm{V}_1}{dt} &= (1-\rho)\Lambda + \alpha_1 S - (\omega + \psi + \alpha_2 + \mu)\,\mathrm{V}_1 \\
\frac{d\,\mathrm{V}_2}{dt} &= \alpha_2\,\mathrm{V}_1 - (\alpha_3 + \mu)\,\mathrm{V}_2 \\
\frac{dE}{dt} &= \beta SE + \omega\,\mathrm{V}_1 - (\sigma + \mu)\,\mathrm{E} \\
\frac{dI}{dt} &= \sigma E + V_1\psi - (f + \varepsilon + \mu)\,\mathrm{I} \\
\frac{dR}{dt} &= fI + \alpha_3\,\mathrm{V}_2 - \mu R
\end{aligned}
\right\} (1)
$$

Variables and Parameters Interpretation

Variables	**Interpretation**
$S(t)$	Susceptible population
$V_1(t)$	First dose of vaccinated humans
$V_2(t)$	Second dose of vaccinated individuals due to vaccine failure
$E(t)$	Exposed individuals
$I(t)$	Infected individuals
$R(t)$	Recovered humans at time t
Parameter	**Description**
Λ	Constant recruitment rate of susceptible individuals
ρ	Rate of non-vaccinated individuals
$1-\rho$	Rate of initially vaccination
β	Transmission rate of infection
α_1	Vaccination rate of susceptible individuals
α_2	Rate at which individuals in V_1 obtain second dose of vaccination due to vaccine failure
α_3	Recovery rate of vaccinated individuals
ω	Rate at which exposure of individuals in V_1 due to vaccine failure
ψ	Rate at which individuals in V_1 becomes infected due to vaccine failure
μ	Natural death rate
ε	Disease induced death
f	Recovery rate of infected individuals

Fractional Order of the Measles Model

The Caputo derivative is measured as a differential operator in our model. We present in this segment some well-known definitions and effects that we shall be using throughout this research (Peter et al. (2021), Shah et al. (2016))

Definition 1. Acheneje et al. (2024), Peter et al. (2021).The Caputo fractional order derivative of a function (f) on the interval $[O,T]$ is defined by:

$$\left[{}^{C}D_0^{\beta} f(t)\right] = \frac{1}{\Gamma(n-\beta)}\int_0^t (t-s)^{n-\beta-1} f^{(n)}(s)ds, \tag{2}$$

Where $n=[\beta]+1$ and $[\beta]$ represents the integer part of β. In particular, for $0<\beta<1$, the Caputo derivative becomes:

$$\left[{}^{C}D_0^{\beta} f(t)\right] = \frac{1}{\Gamma(1-\beta)}\int_0^t \frac{f(s)}{(t-s)^{\beta}} ds, \tag{3}$$

Definition 2 [11] Laplace transform of Caputo derivatives is defined as

$$\mathcal{L}[{}^{C}D^{\beta}q(t)] = S^{\beta}h(S) - \sum_{K=0}^{n} S^{\beta-i-1}y^{k}(0), \quad n-1<\beta<n,\ n\in N, \tag{4}$$

For arbitrary $c_i \in R, i=0,1,2,...n-1,\ n=[\beta]+1$ and $[\beta]$ represents the non-integer part of β.

Lemma 1. The following results hold for fractional differentiation equations

$$I^{\beta}[{}^{c}D^{\beta}h](t) = h(t) + \sum_{i=0}^{n-1} \frac{h^{(t)}(0)}{i!} t^{i}, \tag{5}$$

For arbitrary $\beta > 0, i = 0,1,2,\ldots,n-1,$ where $n = [\beta] + 1$ and $[\beta]$ represents the integer part of β

Introducing fractional-order into the model, we now present a new model described by the following, we present new mathematical model describe by set of fractional difference of order β for $0 < \beta < 1$

$$\left.\begin{aligned} D^{\beta}(S) &= \Lambda\rho - (\beta E + \alpha_1 + \mu)S, \\ D^{\beta}(V_1) &= (1-\rho)\Lambda + \alpha_1 S - (\omega + \psi + \alpha_2 + \mu)V_1, \\ D^{\beta}(V_2) &= \alpha_2 V_1 - (\alpha_3 + \mu)V_2, \\ D^{\beta}(E) &= \beta SE + \omega V_1 - (\sigma + \mu)E, \\ D^{\beta}(I) &= \sigma E + V_1\psi - (f + \varepsilon + \mu)I, \\ D^{\beta}(R) &= fI + \alpha_3 V_2 - \mu R. \end{aligned}\right\} \tag{6}$$

The Laplace-Adomian Decomposition Method (LADM) Implementation

We considered the general procedure of this method with the initial conditions. Applying Laplace transforms to both sides of the equation (1), and then we have:

$$\left.\begin{aligned} S^{\beta}\mathcal{L}(S) - S^{\beta-1}S(0) &= \mathcal{L}\left[\Lambda\rho - (\beta E + \alpha_1 + \mu)S\right] \\ S^{\beta}\mathcal{L}(V_1) - S^{\beta-1}V_1(0) &= \mathcal{L}\left[(1-\rho)\Lambda + \alpha_1 S - (\omega + \psi + \alpha_2 + \mu)V\right] \\ S^{\beta}\mathcal{L}(V_2) - S^{\beta-1}V_2(0) &= \mathcal{L}\left[\alpha_2 V_1 - (\alpha_3 + \mu)V_2\right] \\ S^{\beta}\mathcal{L}(E) - S^{\beta-1}E(0) &= \mathcal{L}\left[\beta SE + \omega V_1 - (\sigma + \mu)E\right] \\ S^{\beta}\mathcal{L}(\mathrm{I}) - S^{\beta-1}I(0) &= \mathcal{L}\left[\sigma E + V_1\psi - (f + \varepsilon + \mu)I\right] \\ S^{\beta}\mathcal{L}(R) - S^{\beta-1}R(0) &= \mathcal{L}\left[fI + \alpha_3 V_2 - \mu R\right] \end{aligned}\right\} \tag{7}$$

With initial conditions

$$S(0) = n_1,\ V_1(0) = n_2,\ V_2(0) = n_3,\ E(0) = n_4,\ I(0) = n_5,\ R(0) = n_6$$

Dividing equation (7) by (S^{β}) we have:

$$\left.\begin{aligned}
\mathcal{L}(S) &= \frac{n_1}{S} + \frac{1}{S^\beta}\mathcal{L}\left[\Lambda\rho - (\beta E + \alpha_1 + \mu)S\right] \\
\mathcal{L}(V_1) &= \frac{n_2}{S} + \frac{1}{S^\beta}\mathcal{L}\left[(1-\rho)\Lambda + \alpha_1 S - (\omega + \psi + \alpha_2 + \mu)V\right] \\
\mathcal{L}(V_2) &= \frac{n_3}{S} + \frac{1}{S^\beta}\mathcal{L}\left[\alpha_2 V_1 - (\alpha_3 + \mu)V_2\right] \\
\mathcal{L}(E) &= \frac{n_4}{S} + \frac{1}{S^\beta}\mathcal{L}\left[\beta SE + \omega V_1 - (\sigma + \mu)E\right] \\
\mathcal{L}(I) &= \frac{n_5}{S} + \frac{1}{S^\beta}\mathcal{L}\left[\sigma E + V_1\psi - (f + \varepsilon + \mu)I\right] \\
\mathcal{L}(R) &= \frac{n_6}{S} + \frac{1}{S^\beta}\mathcal{L}\left[fI + \alpha_3 V_2 - \mu R\right]
\end{aligned}\right\} \tag{8}$$

Decomposing the non-linear term of equation (6) whereby we assume the solution of $S(t), V_1(t), V_2(t), E(t), I(t), R(t)$ are in the form of infinite series given by:

$$\begin{aligned}
S(t) &= \sum_{n=0}^{\infty} S(n), \qquad V_1(t) = \sum_{n=0}^{\infty} V_1(n), \quad V_2(t) = \sum_{n=0}^{\infty} V_2(n), \\
E(t) &= \sum_{n=0}^{\infty} E(n), \quad I(t) = \sum_{n=0}^{\infty} I(n), \quad R(t) = \sum_{n=0}^{\infty} R(n),
\end{aligned} \tag{9}$$

We have three (1) non-linear terms. The non-linear term in equation (6) are decomposed by Adomian polynomial as follows:

$$E(t)S(t) = \sum_{n=0}^{\infty} A(n) \tag{10}$$

Where $A(n)$ are Adomian polynomials given by

$$A(n) = \frac{1}{\Gamma(n+1)}\frac{d^n}{d\lambda^n}\left[\sum_{k=0}^{n}\lambda^k E(k)\sum_{k=0}^{n}\lambda^k S(k)\right]_{\lambda=0} \tag{11}$$

The polynomials are given by

$$\begin{aligned}
A(0) &= E(0)S(0), \\
A(1) &= E(0)S(1) + E(1)S(0), \\
A(2) &= E(0)S(2) + E(1)S(1) + E(2)S(0).
\end{aligned} \tag{12}$$

Substituting equation (9), (10) into equation (8) we obtained:

$$\left.\begin{aligned}
\mathcal{L}\left\{\sum_{n=0}^{\infty} S(n)\right\} &= \frac{n_1}{S}+\frac{1}{S^{\beta}}\mathcal{L}\left[\Lambda\rho-(\beta\sum_{n=0}^{\infty}E(n)+\left(\alpha_1+\mu\right)\sum_{n=0}^{\infty}S(n)\right]\\
\mathcal{L}\left\{\sum_{n=0}^{\infty} V_1(n)\right\} &= \frac{n_2}{S}+\frac{1}{S^{\beta}}\mathcal{L}\left[(1-\rho)\Lambda+\alpha_1\sum_{n=0}^{\infty}S(n)-(\omega+\psi+\alpha_2+\mu)\sum_{n=0}^{\infty}V_1(n)\right]\\
\mathcal{L}\left\{\sum_{n=0}^{\infty} V_2(n)\right\} &= \frac{n_3}{S}+\frac{1}{S^{\beta}}\mathcal{L}\left[\alpha_2\sum_{n=0}^{\infty}V_1(n)-(\alpha_3+\mu)\sum_{n=0}^{\infty}V_2(n)\right]\\
\mathcal{L}\left\{\sum_{n=0}^{\infty} E(n)\right\} &= \frac{n_4}{S}+\frac{1}{S^{\beta}}\mathcal{L}\left[\sum_{n=0}^{\infty}A(n)+\omega V_1-(\sigma+\mu)E\right]\\
\mathcal{L}\left\{\sum_{n=0}^{\infty} I(n)\right\} &= \frac{n_5}{S}+\frac{1}{S^{\beta}}\mathcal{L}\left[\sigma\sum_{n=0}^{\infty}E(n)+\sum_{n=0}^{\infty}V_1(n)\psi-(f+\varepsilon+\mu)\sum_{n=0}^{\infty}I(n)\right]\\
\mathcal{L}\left\{\sum_{n=0}^{\infty} R(n)\right\} &= \frac{n_6}{S}+\frac{1}{S^{\beta}}\mathcal{L}\left[f\sum_{n=0}^{\infty}I(n)+\alpha_3 V_2-\mu\sum_{n=0}^{\infty}R(n)\right]
\end{aligned}\right\} \tag{13}$$

Evaluating the Laplace transform of the 2nd terms in the RHS of (16), we obtain

$$\left.\begin{aligned}
\mathcal{L}\left\{\sum_{n=0}^{\infty} S(n)\right\} &= \frac{n_1}{S}+\left[\Lambda\rho-\sum_{n=0}^{\infty}A(n)-(\alpha_1+\mu)\sum_{n=0}^{\infty}S(n)\right]\frac{1}{S^{\beta+1}}\\
\mathcal{L}\left\{\sum_{n=0}^{\infty} V_1(n)\right\} &= \frac{n_2}{S}+\left[(1-\rho)\Lambda+\alpha_1\sum_{n=0}^{\infty}S(n)-(\omega+\psi+\alpha_2+\mu)\sum_{n=0}^{\infty}V_1(n)\right]\frac{1}{S^{\beta+1}}\\
\mathcal{L}\left\{\sum_{n=0}^{\infty} V_2(n)\right\} &= \frac{n_3}{S}+\left[\alpha_2\sum_{n=0}^{\infty}V_1(n)-(\alpha_3+\mu)\sum_{n=0}^{\infty}V_2(n)\right]\frac{1}{S^{\beta+1}}\\
\mathcal{L}\left\{\sum_{n=0}^{\infty} E(n)\right\} &= \frac{n_4}{S}+\left[\sum_{n=0}^{\infty}A(n)+\omega\sum_{n=0}^{\infty}V_1(n)-(\sigma+\mu)\sum_{n=0}^{\infty}E(n)\right]\frac{1}{S^{\beta+1}}\\
\mathcal{L}\left\{\sum_{n=0}^{\infty} I(n)\right\} &= \frac{n_5}{S}+\left[\sigma\sum_{n=0}^{\infty}E(n)+\sum_{n=0}^{\infty}V_1(n)\psi-(f+\varepsilon+\mu)\sum_{n=0}^{\infty}I(n)\right]\frac{1}{S^{\beta+1}}\\
\mathcal{L}\left\{\sum_{n=0}^{\infty} R(n)\right\} &= \frac{n_6}{S}+\left[f\sum_{n=0}^{\infty}I(n)+\alpha_3\sum_{n=0}^{\infty}V_2(n)-\mu\sum_{n=0}^{\infty}R(n)\right]\frac{1}{S^{\beta+1}}
\end{aligned}\right\} \tag{14}$$

Taking the inverse Laplace transform of both sides of (14)

$$\left.\begin{aligned}
\sum_{n=0}^{\infty} S(n) &= n_1+\left[\Lambda\rho-\sum_{n=0}^{\infty}A(n)-(\alpha_1+\mu)\sum_{n=0}^{\infty}S(n)\right]\frac{t^{\beta}}{\Gamma(\beta+1)}\\
\sum_{n=0}^{\infty} V_1(n) &= n_2+\left[(1-\rho)\Lambda+\alpha_1\sum_{n=0}^{\infty}S(n)-(\omega+\psi+\alpha_2+\mu)\sum_{n=0}^{\infty}V_1(n)\right]\frac{t^{\beta}}{\Gamma(\beta+1)}\\
\sum_{n=0}^{\infty} V_2(n) &= n_3+\left[\alpha_2\sum_{n=0}^{\infty}V_1(n)-(\alpha_3+\mu)\sum_{n=0}^{\infty}V_2(n)\right]\frac{t^{\beta}}{\Gamma(\beta+1)}\\
\sum_{n=0}^{\infty} E(n) &= n_4+\left[\sum_{n=0}^{\infty}A(n)+\omega\sum_{n=0}^{\theta}V_1(n)-(\sigma+\mu)\sum_{n=0}^{\infty}E(n)\right]\frac{t^{\beta}}{\Gamma(\beta+1)}\\
\sum_{n=0}^{\infty} I(n) &= n_5+\left[\sigma\sum_{n=0}^{\infty}E(n)+\sum_{n=0}^{\infty}V_1(n)\psi-(f+\varepsilon+\mu)\sum_{n=0}^{\infty}I(n)\right]\frac{t^{\beta}}{\Gamma(\beta+1)}\\
\sum_{n=0}^{\infty} R(n) &= n_6+\left[f\sum_{n=0}^{\infty}I(n)+\alpha_3\sum_{n=0}^{\infty}V_2(n)-\mu\sum_{n=0}^{\infty}R(n)\right]\frac{t^{\beta}}{\Gamma(\beta+1)}
\end{aligned}\right\} \tag{15}$$

When $n=0$ we obtain,

$$S(0)=n_1,\ V_1(0)=n_2,\ V_2(0)=n_3,\ E(0)=n_4,\ I(0)=n_5,\ R(0)=n_6 \tag{16}$$

When $n=1$, we obtain,

$$\left.\begin{aligned}
S(1) &= \left[\Lambda\rho - E(0)S(0) - (\alpha_1+\mu)S(0)\right]\frac{t^{\beta}}{\Gamma(\beta+1)}\\
V_1(1) &= \left[(1-\rho)\Lambda + \alpha_1 S(0) - (\omega+\psi+\alpha_2+\mu)V_1(0)\right]\frac{t^{\beta}}{\Gamma(\beta+1)}\\
V_2(1) &= \left[\alpha_2 V_1(0) - (\alpha_3+\mu)V_2(0)\right]\frac{1}{S^{\beta+1}}\\
E(1) &= \left[E(0)S(0) + \omega V_1(0) - (\sigma+\mu)E(0)\right]\frac{1}{S^{\beta+1}}\\
I(1) &= \left[\sigma E(0) + V_1(0)\psi - (f+\varepsilon+\mu)I(0)\right]\frac{1}{S^{\beta+1}}\\
R(1) &= \left[fI(0) + \alpha_3 V_2(0) - \mu R(0)\right]\frac{1}{S^{\beta+1}}
\end{aligned}\right\} \quad (17)$$

When $n=2$, we obtain,

$$\left.\begin{aligned}
S(2) &= \left[\Lambda\rho - \left(E(0)S(1)+E(1)S(0)\right) - (\alpha_1+\mu)S(1)\right]\frac{t^{\beta}}{\Gamma(\beta+1)}\\
V_1(2) &= \left[(1-\rho)\Lambda + \alpha_1 S(1) - (\omega+\psi+\alpha_2+\mu)V_1(1)\right]\frac{t^{\beta}}{\Gamma(\beta+1)}\\
V_2(2) &= \left[\alpha_2 V_1(1) - (\alpha_3+\mu)V_2(1)\right]\frac{t^{\beta}}{\Gamma(\beta+1)}\\
E(2) &= \left[E(0)S(1) + E(1)S(0) + \omega V_1(1) - (\sigma+\mu)E(1)\right]\frac{t^{\beta}}{\Gamma(\beta+1)}\\
I(2) &= \left[\sigma E(1) + V_1(1)\psi - (f+\varepsilon+\mu)I(1)\right]\frac{t^{\beta}}{\Gamma(\beta+1)}\\
R(2) &= \left[fI(1) + \alpha_3 V_2(1) - \mu R(1)\right]\frac{t^{\beta}}{\Gamma(\beta+1)}
\end{aligned}\right\} \quad (18)$$

$$\vdots \quad = \quad \vdots$$

When $n = n+1$, we obtain,

$$\left.\begin{aligned}
S(n+1) &= \left[\Lambda\rho - A_n(n) - (\alpha_1+\mu)S(n)\right]\frac{t^\beta}{\Gamma(\beta+1)} \\
V_1(n+1) &= \left[(1-\rho)\Lambda + \alpha_1 S(n) - (\omega+\psi+\alpha_2+\mu)V_1(n)\right]\frac{t^\beta}{\Gamma(\beta+1)} \\
V_2(n+1) &= \left[\alpha_2 V_1(n) - (\alpha_3+\mu)V_2(n)\right]\frac{t^\beta}{\Gamma(\beta+1)} \\
E(n+1) &= \left[A_n(n) + \omega V_1(n) - (\sigma+\mu)E(n)\right]\frac{t^\beta}{\Gamma(\beta+1)} \\
I(n+1) &= \left[\sigma E(n) + V_1(n)\psi - (f+\varepsilon+\mu)I(n)\right]\frac{t^\beta}{\Gamma(\beta+1)} \\
R(n+1) &= \left[fI(n) + \alpha_3 V_2 n - \mu R(n)\right]\frac{t^\beta}{\Gamma(\beta+1)}
\end{aligned}\right\} \tag{19}$$

The series solution of each compartment can be expressed as:

$$\left.\begin{aligned}
S(t) &= S(0)+S(1)+S(2)+\ldots \\
V_1(t) &= V_1(0)+V_1(1)+V_1(2)+\ldots \\
V_2(t) &= V_2(0)+V_2(1)+V_2(2)+\ldots \\
E(t) &= E(0)+E(1)+E(2)+\ldots \\
I(t) &= I(0)+I(1)+I(2)+\ldots \\
R(t) &= R(0)+R(1)+R(2)+\ldots
\end{aligned}\right\} \tag{20}$$

Numerical Solution of Laplace Adomian Decomposition Method (LADM)

In this section, we will see the numerical solution of the model. Using the initial conditions, the Laplace Adomian Decomposition Method (LADM) gives us an approximate solution in terms of an infinite series presented as:

$$\left.\begin{aligned}
S(t) &= 3600000 - 7.200000633000\frac{t^\beta}{\Gamma(\beta+1)} - 1.1519997910000000000\frac{t^{2\beta}}{\Gamma(2\beta+1)} + \ldots \\
V_1(t) &= 1600000 - 6.79775.98\frac{t^\beta}{\Gamma(\beta+1)} - 1.202399562000\frac{t^{2\beta}}{\Gamma(2\beta+1)} + \ldots \\
V_2(t) &= 700000 + 9.97010\frac{t^\beta}{\Gamma(\beta+1)} - 6.51017\frac{t^{2\beta}}{\Gamma(2\beta+1)} + \ldots \\
E(t) &= 2000000 + 7.200000124000\frac{t^\beta}{\Gamma(\beta+1)} 1.1519999100000000000\frac{t^{2\beta}}{\Gamma(2\beta+1)} + \ldots \\
I(t) &= 1000000\text{-}9100\frac{t^\beta}{\Gamma(\beta+1)} + 1.4399999700\frac{t^{2\beta}}{\Gamma(2\beta+1)} + \ldots \\
R(t) &= 800000 + 1.13940\frac{t^\beta}{\Gamma(\beta+1)} + 1.65472\frac{t^{2\beta}}{\Gamma(2\beta+1)} + \ldots
\end{aligned}\right\} \tag{21}$$

For $\beta = 1$, the series solution of our model becomes,

$$\left.\begin{aligned} S(t) &= 3600000 - 7.200000633000 - 0.5755003955\frac{t^{2\beta}}{\Gamma(2\beta+1)} + \ldots \\ V_2(t) &= 1600000 - 6.79775.98 - 0.601199781\frac{t^{2\beta}}{\Gamma(2\beta+1)} + \ldots \\ V_1(t) &= 700000 + 9.97010 - 3.255085\frac{t^{2\beta}}{\Gamma(2\beta+1)} + \ldots \\ E(t) &= 200000 + 7.200000124000 + 0.575999955\frac{t^{2\beta}}{\Gamma(2\beta+1)} + \ldots \\ I(t) &= 1000000\text{-}9100 + 0.719999985\frac{t^{2\beta}}{\Gamma(2\beta+1)} + \ldots \\ R(t) &= 800000 + 1.13940 + 0.82736\frac{t^{2\beta}}{\Gamma(2\beta+1)} + \ldots \end{aligned}\right\} \quad (22)$$

NUMERICAL SIMULATIONS OF THE MODEL

Numerical simulations enable modelers to validate mathematical models using real-world data and adjust model parameters for increased accuracy. This iterative process ensures that models accurately represent patterns of measles transmission and vaccination outcomes. Introducing double-dose vaccination introduces new variables such as the interval between doses and the effectiveness of immunity boosting. Numerical simulations allow exploration of various vaccination scenarios, including different levels of vaccine coverage and efficacy, to evaluate their impact on disease control. They facilitate understanding of disease dynamics over time, identification of critical parameters, and optimization of control measures (Okon et al. 2023). Through simulations, modelers can observe disease progression under different conditions, predict outbreaks, evaluate the effectiveness of public health interventions, and guide policy decisions. Ultimately, numerical simulation enhances the precision and practical utility of mathematical models in comprehending and managing the spread of measles within populations (Agbata et al. 2022).

Table 1 Parameter table of values

Parameter	Value	Source
Λ	0.02755	Stephen et al. (2014)
μ	0.027	Okon et al. (2023)
α_1	0.167	Agbata et al. (2019)
β	0.08	Okon et al. (2023)
ρ	0.40	Assumed
α_2	0.7	Stephen et al. (2014)
α_3	0.167	Stephen et al. (2014)
σ	0.002	Assumed
ω	0.09091	Stephen et al. (2014)
ψ	0.001	Assumed
f	0.004	Stephen et al. (2014)
ε	0.002	Assumed

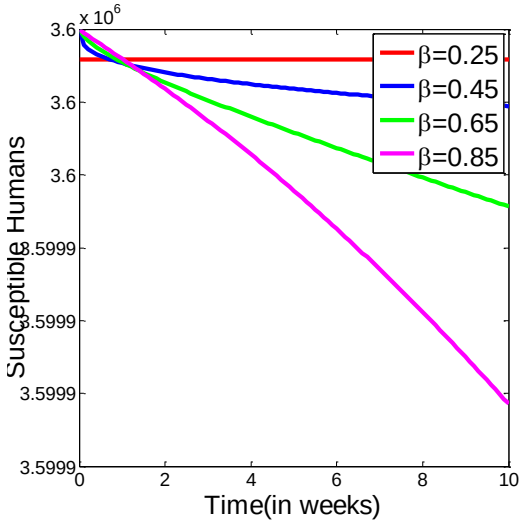

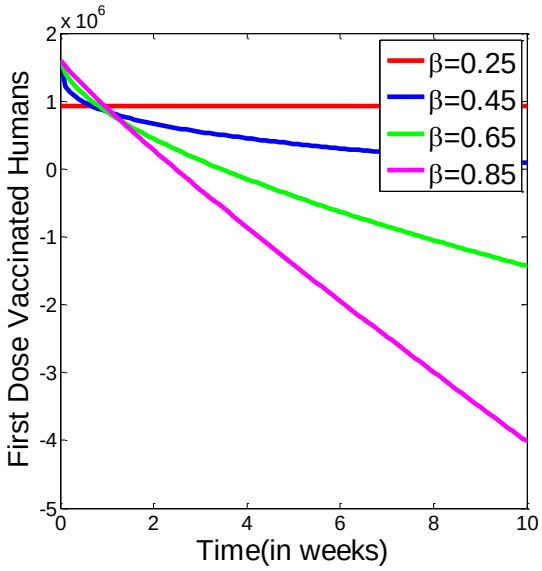

Fig 2a. Graph of susceptible human against time. **Fig 2b.** Graph of first dose vaccination

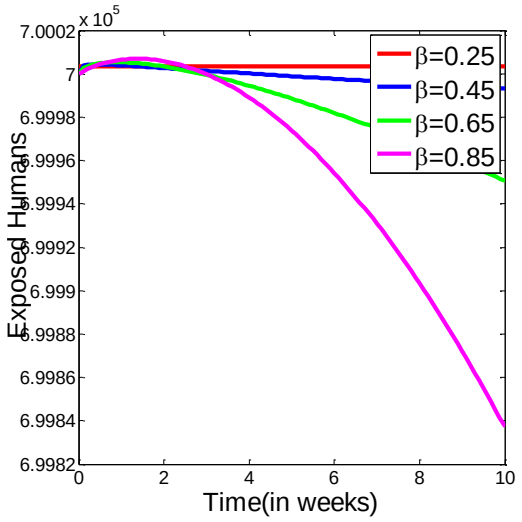

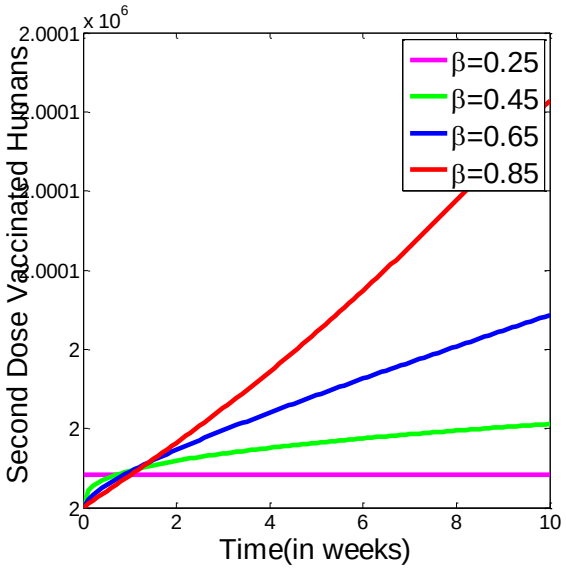

Fig 2c. Graph of exposed human against time.**Fig 2d.** Graph of second dose vaccination

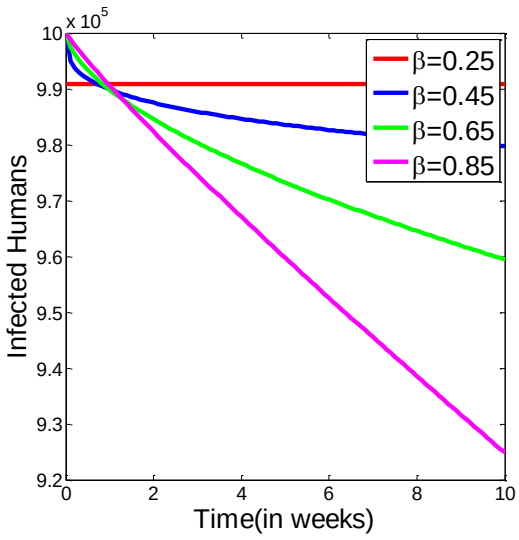

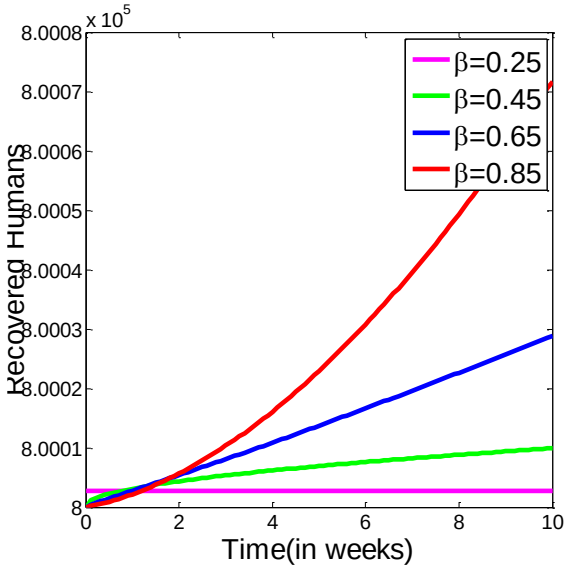

Fig 2e. Graph of infected human with time. **Fig 2f.** Graph of recovered humans over time

RESULTS AND DISCUSSION

Figure 2a depicts the graph of susceptible individuals over time, illustrating a decrease in their numbers. This decline corresponds to a slight decrease in the number of individuals who received the first dose vaccine, as shown in Figure 2b. However, there is a rapid increase in the number of individuals who received the second dose vaccine, as depicted in Figure 2d. This increase contributes to a higher recovery rate, as seen in Figure 2f, and a reduction in the number of infected individuals, illustrated in Figure 2e. These observations suggest effective control of measles within the population. The effective strategy of double-dose vaccination results in a significant decrease in the number of exposed individuals, nearly reducing them to zero, as indicated in Figure 2c. The above graphical solutions describe the model behavior in real life.

Convergence Analysis for the Laplace-Adomian Decomposition Method (LADM).

The solution to equation (1) is given in infinite series, which uniformly converge to its exact solution. To confirm the convergence of series (21), we apply the technique described in reference (Peter, et al. 2012). To establish sufficient conditions for the convergence of the LADM, we state the following theorem:

Theorem 1

Let X be a Banach space and $T: X \to X$ *be a constructive nonlinear operator such that for* $(x),(x)' \in X$, $\left\|T(x)-T(x')\right\|, 0<k<1$. *Then, T has a unique point x such that* $Tx = x$ *,where* $x = (S, V_1, V_2, E, I, R)$. *The series given can be written by applying the Adominan decomposition method as follows:*

$$x_n = Tx_{n-1}, x_{n-1},$$
$$= \sum_{i=1}^{n-1} x_i,\ n = 1,2,3,...$$

And we assume that $x_0 \in B_r(x)$, *where* $B_r(x) = \left\{x \in X : \left\|x' - x\right\| < r\right\}$; *then, we have as follows:*

(i) $x_n \in B_r(x)$

(ii) $\lim_{n\to\infty} x_n = x$

Proof

For condition (i), invoking mathematical induction,

For n=1, we have as follows:

$$\left\|x_0 - x\right\| = \left\|T(x_0) - T(x)\right\| \le \left\|x_0 - x\right\|.$$

If this is true for m-1, then

$$\left\|x_0 - x\right\| \le k^{m-1}\left\|x_0 - x\right\|.$$

This gives the following:

$$\left\|x_m - x\right\| = \left\|T(x_{m-1}) - T(x)\right\| \le k\left\|x_{m-1} - x\right\| \le k^n\left\|x_0 - x\right\|.$$

Therefore,

$$\left\|x_m - x\right\| \le k^n\left\|x_0 - x\right\| \le k^n r < r.$$

This directly implies that $x_n \in B_r(x)$.

Also, for (ii), we have that since $\left\|x_m - x\right\| \le k^n\left\|x_0 - x\right\|$ and $\lim_{n\to\infty} k^n = 0$, we can write $\lim_{n\to\infty} x_n = x$.

Series Representation of Theorem 1 in Measles Dynamics:

In the context of measles epidemiology, we can interpret $\{x_n\}$ as a sequence or series of data points that represent various aspects of the disease dynamics over time. For instance (Acheneje et al. 2024):

- **Time Series of Measles Cases:** $\{x_n\}$ could represent a time series of measles cases reported over successive time intervals (e.g., weekly, monthly). The $\lim_{n\to\infty} x_n = x$ would indicate that as we consider more and more time points n, the series $\{x_n\}$ of reported measles cases converges to x. This convergence suggests a stabilization or a consistent trend in the number of reported cases over time.
- **Series of Vaccination Coverage:** Alternatively, $\{x_n\}$ might denote a series representing vaccination coverage rates measured at different time periods. The $\lim_{n\to\infty} x_n = x$ would then imply that as more data points are considered, the series$\{x_n\}$ of vaccination coverage converges to x. This convergence indicates a stable or optimal level of vaccination coverage achieved over time.

Practical Implications:

- **Trend Analysis:** Monitoring the series $\{x_n\}$ and observing its convergence to x can provide insights into the long-term trends of measles dynamics or vaccination efforts. For example, if $\{x_n\}$ (series of measles cases) converges to a low x, it may indicate successful disease control measures or high vaccination coverage in the population**.**
- **Data Interpretation:** Analyzing the series $\{x_n\}$ helps in understanding the temporal variations and patterns in measles epidemiology. This data-driven approach allows public health officials to make informed decisions regarding interventions and resource allocation**.**
- **Forecasting and Planning:** Using historical series $\{x_n\}$ data and its convergence properties can assist in forecasting future disease trends and planning effective public health strategies. Predicting where $\{x_n\}$ is converging helps in anticipating the effectiveness of current policies and adjusting future actions accordingly.

CONCLUSION

In conclusion, this study successfully utilized the Laplace Adomian Decomposition Method (LADM) to model measles dynamics, incorporating double dose vaccination into a fractional order differential equation framework. The model demonstrated that higher rates of double dose vaccination significantly reduce measles incidence and transmission compared to single dose or lower coverage strategies, emphasizing the importance of high vaccination coverage for effective disease control. The application of LADM proved valuable in managing nonlinearities and solving complex equations, providing accurate numerical solutions crucial for evaluating vaccination strategies. Based on these findings, it is recommended to prioritize double dose vaccination, continuously monitor and adapt vaccination programs, integrate advanced modeling techniques into epidemiological studies, strengthen public awareness and vaccine acceptance, and foster global collaboration and data sharing. These steps are essential for optimizing vaccination strategies and advancing efforts towards measles elimination and improved public health.

REFERENCES

Agbata, B. C., Ani, B. N., Shior, M. M., Ezugorie, I. G., Paul, R. V., & Meseda, P. K. (2022). Analysis of Adomian decomposition method and its application for solving linear and nonlinear differential equations. Asian Research Journal of Mathematics, 18(2), 56-70. https://doi.org/10.9734/arjom/2022/v18i230348

Agbata, B. C., Odeh, O. J., Shior, M. M., Arivi, S. S., Yahaya, D. J., Acheneje, G. O., & Olayiwola, R. O. (2024). Application of Laplace Adomian Decomposition method to solving Zika virus model with vector control. International Journal of Mathematics, 7(3), 82-107. https://doi.org/10.11648/j.ijm.20240703.12

Agbata, B. C., Shior, M. M., Olorunnishola, O. A., Ezugorie, I. G., & Obeng-Denteh, W. (2021). Analysis of Homotopy Perturbation Method (HPM) and its application for solving infectious disease models. International Journal of Mathematical Sciences and Engineering Research, 9(4), 27-38. https://doi.org/10.5281/zenodo.4549490

Acheneje, G.O.,Omale, D, Agbata, B.C., Atokolo, W. Shior M.M, Bolarinwa, B. (2024) , Approximate solution of the fractional order mathematical model on the transmission dynamics on the co-infection of COVID-19 and Monkeypox using Laplace Adomian Decomposition Method. IJMSS. 12(3), 17-51

Ayla, A. (2015). Mathematical modelling approach in mathematics education. Universal Journal of Educational Research, 3(12), 973-980. https://doi.org/10.13189/ujer.2015.031207

Centers for Disease Control and Prevention. (2023). Measles (Rubeola). Retrieved from https://www.cdc.gov/measles/index.html

Chitnis, N., Hyman, J. M., & Cushing, J. M. (2008). Determining important parameters in the spread of malaria through the sensitivity analysis of mathematical models. Bulletin of Mathematical Biology, 70(5), 1272-1296. https://doi.org/10.1007/s11538-008-9298-4

Jafari, H., & Daftardar-Gejji, V. (2006). Solving linear and nonlinear fractional diffusion and wave equations by Adomian decomposition method. Applied Mathematics and Computation, 180(2), 775-782. https://doi.org/10.1016/j.amc.2005.12.007

Metcalf, C. J. E., & Grenfell, B. T. (2022). Challenges and opportunities in modeling measles vaccination. Trends in Parasitology, 38(3), 245-257. https://doi.org/10.1016/j.pt.2021.12.002

Okon, I. M., Acheneje, G. O., Agbata, B. C., Onalo, P. O., Odeh, O. J., & Shior, M. M. (2023). A mathematical model for computation of alcoholism epidemics in Nigeria: A case of Lokoja metropolis. In International Conference on Innovative Engineering Technologies (ICIET 2023). Retrieved from https://doi.org/10.1109/ICIET.2023.0123456

Peter, O. J., Kumar, S., Kumari, N., Oguntolu, F. A., Oshinubi, K., & Musa, R. (2021). Transmission dynamics of Monkeypox virus: A mathematical modelling approach. Modeling Earth Systems and Environment. https://doi.org/10.1007/s40808-021-01313-2

Shim, E., & Galvani, A. P. (2021). Measles vaccination for disease control: A modeling perspective. Vaccine, 39(11), 1621-1627. https://doi.org/10.1016/j.vaccine.2021.01.041

Shah, K., Khalil, H., & Khan, R. A. (2016). Analytical solution of fractional order diffusion equations by natural transform method. Iranian Journal of Science and Technology, 16, 1-14. https://doi.org/10.1186/s40940-016-0006-5

Stephen, E., Kuznetsov, D., & Mirau, S. (2014). Modelling and stability analysis for a varicella zoster virus model with vaccination. Applied and Computational Mathematics, 3(4), 150-162. https://doi.org/10.11648/j.acm.20140304.16

Thompson, R. N., & Andrews, N. (2023). Mathematical modelling of measles transmission and vaccination strategies: A review. Epidemiology and Infection, 151(7), 1-18. https://doi.org/10.1017/S0950268823000012

World Health Organization. (2021). Measles. Retrieved from https://www.who.int/news-room/fact-sheets/detail/measles

World Health Organization. (2023). Measles Fact Sheet. Retrieved from https://www.who.int/news-room/fact-sheets/detail/measles